Exciton dispersion in two-dimensional organic perylene crystal indicates substantial charge-transfer exciton coupling

Lukas Graf and Martin Knupfer
IFW Dresden, Helmholtzstrasse 20, 01069 Dresden, Germany

Qingqing Wang, Mats Fahlman, and Xianjie Liu
Laboratory of Organic Electronics, Department of Science and Technology, Linköping University, 60174 Norrköping, Sweden

(Received 28 November 2022; revised 7 February 2023; accepted 9 February 2023; published 1 March 2023)

Two-dimensional, high-quality perylene single crystals were grown with a space-confined strategy method. The grown films crystallize in the α form, as is confirmed by a combination of techniques. Polarization-dependent optical absorption measurements show a strong anisotropy in very good agreement with the literature data, and the anisotropic mobility data in field-effect transistors document the very high crystalline order. Momentum-dependent studies using electron energy-loss spectroscopy reveal a negative dispersion of the first exciton along the crystal *b* direction with an exciton bandwidth of 72 meV. We argue that this behavior is a result of charge-transfer exciton coupling between the perylene dimers in the unit cell.

DOI: 10.1103/PhysRevB.107.115201

I. INTRODUCTION

Molecular organic semiconductors are an important material class, in that they are chemically tunable, and offer low-cost device processing with the prospect of organic (opto)electronics, with advanced solar cells and light-emitting diodes already being demonstrated [1–5]. Usually, they are bound by noncovalent interactions, which renders their physical properties rather different as compared to conventional semiconductors. This is true for charge carrier transport, as well as for electronic excitations. Frequently, the excited-state properties and thus the photophysics of organic semiconductors are dominated by rather strongly bound excitons. In crystalline materials, exciton coupling between the molecules gives rise to an exciton band structure $E(k)$ from which the basic photophysics can be deduced [6,7]. In contrast to the fundamental importance of the exciton band structure, in the past it has only been determined experimentally for a few organic semiconductors.

In this paper, we present electron energy-loss spectroscopy (EELS) measurements of single-crystalline α-perylene. EELS is well suited to study the energy-momentum relation of electronic excitations in materials [8–10]. Perylene can be considered as a prototypical material as it is the parent molecule for a large class of organic dyes. In the α-polymorph, it crystallizes in a special arrangement, with two molecules forming a dimer, which are then ordered in a herringbone structure [11,12]. α-perylene is therefore an interesting archetype system, as different molecular interactions may lead to complex photophysical behavior [13,14]. Prior studies of α-perylene single crystals have revealed a strongly anisotropic optical response in the crystal *ab* plane, and the corresponding data have mainly been interpreted based upon the Coulomb coupling of the molecular excitons and their interaction with molecular vibrations [13–20]. However, the exciton's energy-momentum characteristics have not yet been reported.

In order to obtain high-quality single crystals of α-perylene for our studies, we have used a space-confined strategy [21] which was proposed recently in order to grow so-called two-dimensional (2D) organic crystals. These 2D organic crystals [22], defined as a class of materials with a periodic arrangement of mono- or multilayers of molecules in a 2D plane, have emerged as an important and hot topic in the research field of optoelectronic and 2D materials in general. 2D organic crystals feature unique characteristics such as long-range ordered packing, a few grain boundaries, as well as minimum defects and traps, offering deep insight into the intrinsic optoelectronic properties that enable the fabrication of high-performance optoelectronic devices [23,24].

Our results reveal a negative exciton dispersion in α-perylene for momenta parallel to the crystal *b* axis. We argue that this cannot be rationalized based upon Coulomb exciton coupling only. Within an effective model that considers the coupling between perylene dimers in the unit cell only, we propose an additional charge-transfer coupling between the excitons on the dimers of about 20 meV.

II. EXPERIMENTAL AND SAMPLE CHARACTERIZATION

A high-quality single-crystalline film is crucial for the investigations. 2D organic crystals of perylene were obtained, based on a space-confined method [21] by dropping 50 µl of perylene chlorobenzene solution with a concentration of 0.5 mg/ml on de-ionized water with a tetrabutylammonium bromide concentration of 10 mg/ml. After the solvent was evaporated, 2D perylene crystals formed on the water surface. The as-grown 2D crystals were transferred onto standard

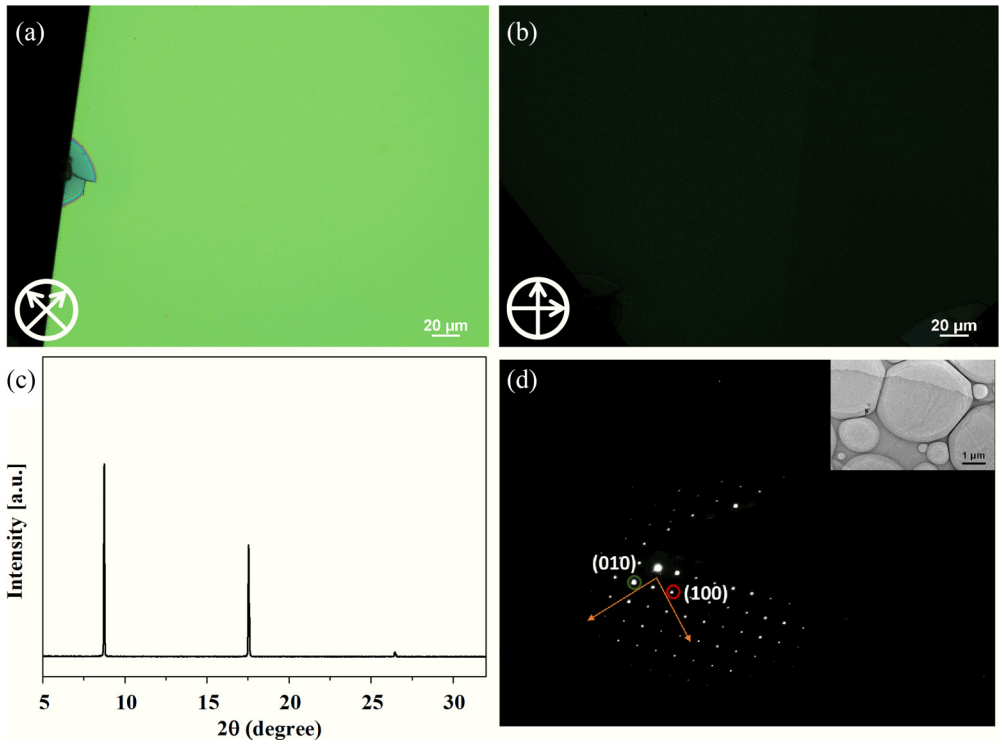

FIG. 1. Structural information about the grown perylene 2D organic semiconductor (2DOSC): (a) and (b) Cross POM images in two perpendicular directions. (c) XRD diffraction pattern. (d) SAED pattern with the corresponding TEM image shown in the inset.

transmission electron microscopy (TEM) grids as a free-standing film, or on SiO_2/Si, followed by vacuum annealing at 353 K for 12 h to remove any contamination. This transfer can be easily achieved by inserting the substrate at an angle into the water [25]. The following annealing process only aims to remove the residual water on the crystal surface, which is usually performed with a relatively slow heating rate and low temperature, i.e., 0.2°/min up to 80 °C. The quality of the 2D organic crystal perylene was examined by various methods, e.g., optical spectroscopy, x-ray diffraction, and transmission electron microscopy (TEM) equipped with selected-area electron diffraction (SAED). To evaluate the crystal quality of the 2D crystal of perylene, we employed cross-polarized optical microscopy (POM), x-ray diffraction (XRD), and TEM with SAED. The corresponding results are shown in Fig. 1. The POM images of a perylene crystal transferred to an SiO_2/Si substrate are presented in Figs. 1(a) and 1(b). They demonstrate a uniform light extinction over the whole crystal which indicates the high-quality single-crystalline nature of the 2D organic crystal. It is well known that perylene crystallizes in two monoclinic polymorphs with $P2_1/c$ symmetry: The α form [11,12] is defined by a close π stacking of two molecules into a dimer, which are then packed in a herringbone structure. The crystal structure of the β form [12,15] is a monomeric herringbone structure. The XRD pattern of our 2D crystal on SiO_2/Si is depicted in Fig. 1(c). It reveals diffraction peaks at $2\theta = 8.738^\circ$, 17.538°, and 26.447°, which correspond very well with the (00l) peaks of α-perylene [11,12] with a layer spacing of 10.109 Å. In addition, the sharp intense peaks and the straight baseline demonstrate the high quality of our grown 2D organic crystal perylene. For more detailed structure information about the smooth crystal of perylene [see the inset of Fig. 1(d)], TEM with a SAED pattern was measured, as shown in Fig. 1(d). The SAED pattern can be indexed according to the α form, clearly indicating the two main directions of [100] and [010] within the 2D plane. The lattice constants calculated from this pattern are $\boldsymbol{a} = 11.09$ Å and $\boldsymbol{b} = 10.76$ Å, which are very well consistent with the reported values [11,12,25]. Thus, all results confirm the high quality of our 2D crystals of α-perylene.

To further elucidate the crystallinity of the 2D crystals of α-perylene, the intrinsic anisotropy of charge transport has been investigated. The 2D organic perylene crystals are transferred to heavily n-type doped SiO_2(100 nm)/Si substrates with octadecyl trichlorosilane (OTS) modification to fabricate organic field-effect transistors (OFETs), in which the bottom-gate top-contact structure was formed by stamping Au (120 nm) stripes on the surface of the perylene crystal as the source and drain electrodes. Prior to the OTS modification, the substrate was successively cleaned by de-ionized water, Piranha solution (70/30 vol%/vol% H_2SO_4/H_2O_2), de-ionized water, acetone, and isopropanol, then treated with oxygen plasma at 50 W for 15 min [26]. The hole mobility in the OFET in the saturation regime is obtained from the equation $I_{DS} = (W/2L)\mu C_i(V_{GS} - V_{th})^2$, where I_{DS} is the source-drain current, μ is the field-effect mobility, V_{th} is the threshold voltage, V_{GS} is the applied gate voltage, W/L is the ratio of channel width and length, and C_i is the specific capacitance (30 nF cm^2). The obtained typical transfer and output curves along the [100] and [010] direction of the 2D α-perylene crystals are shown in Fig. 2. We obtained a higher mobility along the [100] direction ($\mu = 2.59 \times 10^{-2}$ cm^2 V^{-1} s^{-1}) than in the [010] direction ($\mu = 1.25 \times 10^{-2}$ cm^2 V^{-1} s^{-1}), which can be attributed to

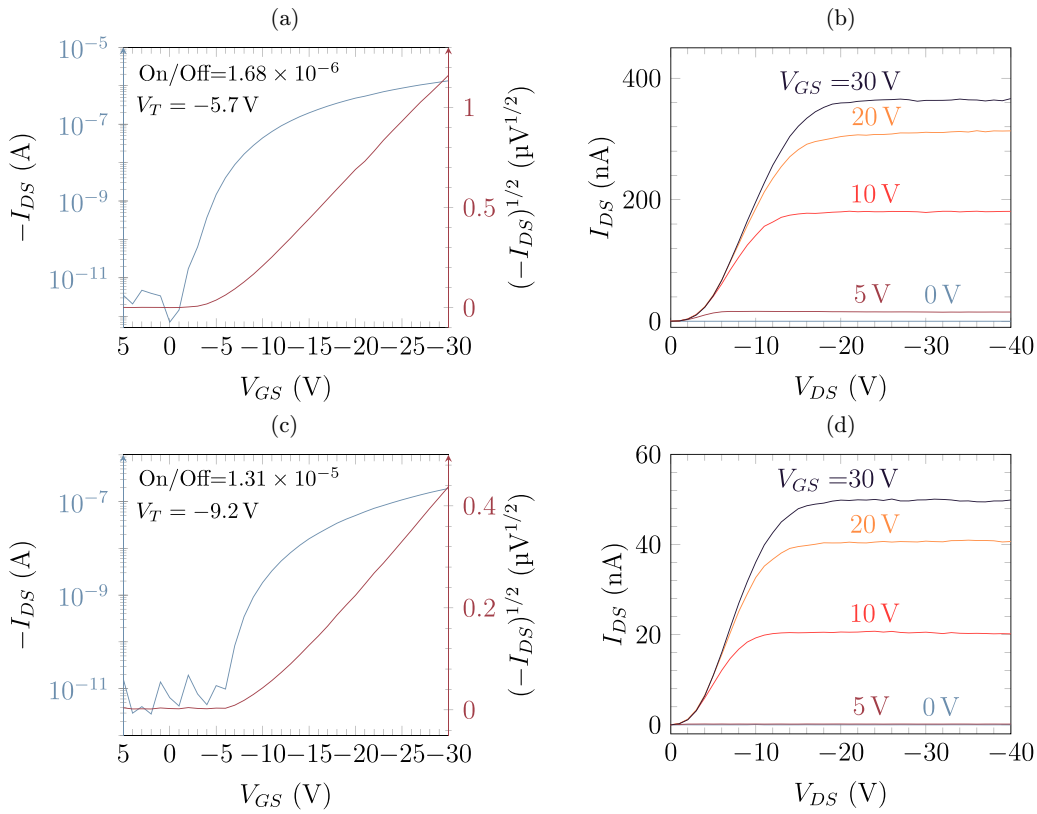

FIG. 2. Typical transfer and output curves of 2D α-perylene crystal OFET devices measured (a), (b) along the [100] direction and (c), (d) along the [010] direction.

the more densely packed molecules in this crystal direction. The anisotropy of the mobility along the two crystal directions is about 1.63, as obtained by averaging the results from seven different devices, which is well consistent with the reported values [27,28] and underlines the very high crystallinity of our 2D α-perylene.

Finally, prior to the EELS measurements every crystal placed on the TEM grid was analyzed with electron diffraction in the EELS spectrometer to confirm the crystallinity of the actual sample and to determine the direction of momentum transfer with respect to the crystal axes. A representative diffraction pattern of both in-plane directions [100] and [010] is shown in Fig. 3. Figure 3 clearly demonstrates the crystalline structure of the EELS samples, with the two patterns agreeing very well with the crystal structure of α-perylene [11,12].

For optical absorption measurements, perylene crystals on TEM grids were measured using a Bruker vertex spectrometer in the UV-VIS range at 77 K. Electron diffraction and EELS were performed with a custom-made electron energy-loss spectrometer, which can detect electronic excitations as a function of momentum transfer [29,30]. The primary electron energy was 172 keV. To keep organic single crystals undamaged as long as possible, the sample temperature was always kept at 20 K, which also minimized thermal broadening in the spectra. Every sample was checked regularly for sample degradation to avoid distorted data. Electron diffraction was applied *in situ* prior to every measurement to ensure the quality of the sample and conformance with the perylene crystal structure (see Fig. 3). With an energy and momentum resolution of about 85 meV and 0.035 Å^{-1}, the measured signal in EELS is proportional to the loss function Im$[-1/\epsilon(q,\omega)]$ and can be determined for different momentum transfers q. By increasing the momentum transfer value q, the EELS cross section decreases proportionally to $\sim q^{-2}$. To obtain a similar signal-to-noise ratio, longer measurement times are needed.

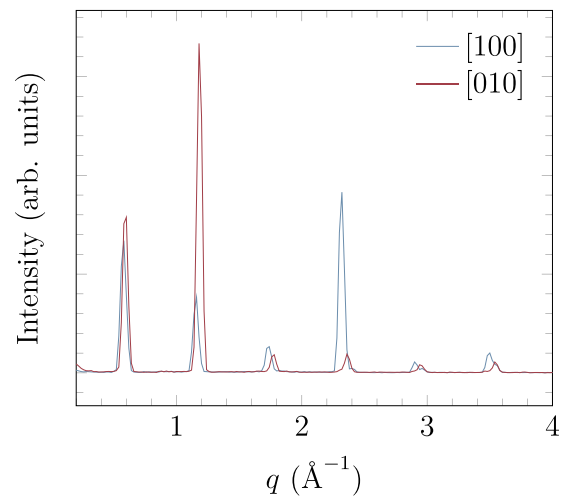

FIG. 3. Electron diffraction pattern of the two in-plane directions [100] and [010] of perylene single crystals as a function of momentum as measured using the EELS spectrometer.

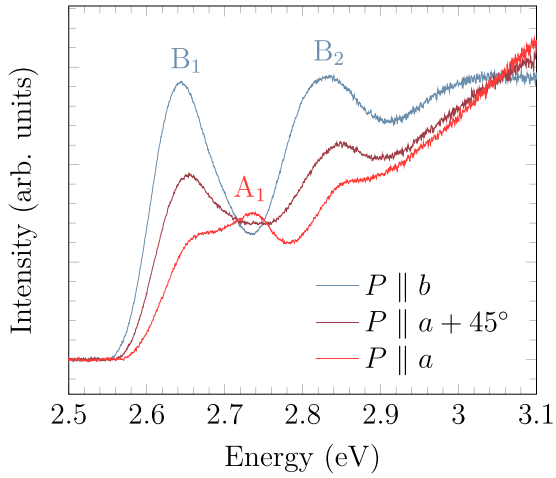

FIG. 4. Polarization (P)-dependent optical absorption measurements of 2D perylene single crystals for light polarizations parallel to the crystal's a and b direction.

III. ELECTRONIC EXCITATIONS IN THE OPTICAL LIMIT

We start with the presentation of the polarization-dependent optical absorption data, measured at 77 K and given in Fig. 4. Three different polarization directions of the incoming light with respect to the crystal directions are shown. These were determined by a comparison of the optical data to those from EELS, where electron diffraction was additionally possible (see above). The blue curve in Fig. 4 is measured with a polarization vector parallel to the b axis, the red curve represents a light polarization parallel to the a axis, and the purple curve is measured at 45° between both directions, to visualize the change between both axes.

The curve for light polarization parallel to the b axis shows the first feature B_1 with an onset at 2.55 eV and peak position at 2.645 eV. This first singlet excitation is followed by a second peak B_2 at 2.83 eV, which can be assumed to be of a vibrational origin as the Raman [31] and solution data indicate [15]. Going to the a-axis spectrum, the absorption intensity at the spectral onset decreases and a new feature A_1 shows up at 2.74 eV. We emphasize that these absorption data are in very good agreement with the data in the literature [14–16].

We now briefly recall how the optical absorption data of α-perylene single crystals have been rationalized in the literature [13,16,17]. The perylene dimers in the crystal structure allow for a quite substantial dipole-dipole coupling in the excited state, whereas the coupled transition dipole moments are parallel to the long molecular axis and quite close to each other. This coupling results in two split dimer states, whereas the energetically lower one is optically forbidden. Coulomb coupling between the dimers in the crystal further splits the allowed state, giving rise to two absorption features at different energies and with polarizations along the a and b axis. The associated energy splitting explains our spectral features B_1 and A_1, with an energy difference of about 92 meV which would be the Davydov splitting. Also, based on the crystal structure and this coupling scheme, it was proposed that from a spectral point of view it is quite accurate to regard the α-perylene crystal to consist of two dimers in the unit cell which couple via the mentioned interdimer coupling. The two dimers then are characterized by a quite strong transition dipole moment, about twice a large as that of the individual molecules because of the coupling of the parallel molecules in a dimer.

IV. EXCITON DISPERSION

Knowledge of the exciton dispersion is important for a full understanding of the photophysical behavior of a material and it has been directly determined for only a couple of organic semiconductor materials in the past. Following the above-mentioned description of the excited states in α-perylene, the excited-state dispersion or exciton band structure could be derived. The transition dipole moment of the two dimers in the unit cell can be estimated to be about twice that of the individual molecule, and the latter results from the reported oscillator strength of $f = 0.3088$ [32] and a transition energy of 2.64 eV [32] to about 5.6 D. Using a point-dipole approximation [33] and a static dielectric constant of $\epsilon_S = 3.25$ [14], the interdimer exciton Coulomb coupling J_C can be estimated to be 49 meV. From the experimentally observed Davydov splitting ($8J_C = 92$ meV, see above), a somewhat smaller value of 11.5 meV would follow. The difference of these values notwithstanding, J_C is positive, in agreement with the parallel arrangement of the transition dipoles. The exciton energies of the coupled dimer states, i.e., the exciton dispersion, now would be

$$E(q) = E_0 \pm 4J_C \cos\left(\frac{qa}{2}\right)\cos\left(\frac{qb}{2}\right), \tag{1}$$

where a and b are the two lattice vectors, and q is the momentum vector. Thus, the positive value of J_C causes the energetically lower state to have a positive exciton dispersion (shift to higher energies upon increasing momentum q).

In Fig. 5(a) we present the measured momentum dependence of the electronic excitations in α-perylene for momenta parallel to the crystal b axis up to 0.5 Å^{-1}. These data demonstrate a clear dispersion of the first excitation B_1 towards lower energies. Also, the second peak B_2 disperses to lower energies in a similar manner, which is in agreement with the assumption written above, that it is of a vibronic nature. In order to extract the exciton dispersion quantitatively, we have fitted the low-energy peaks for all momenta using a Gaussian model to determine the exact peak position (see Supplemental Material [34]). These are given in Fig. 5(b) and display a clear downshift of the first peak from 2.74 to 2.68 eV, in contrast to our expectation above, based on Coulomb coupling between the two perylene dimers in the unit cell. In order to extract the dimer coupling as observed in the experiment within the model outlined above, we have modeled the exciton dispersion as seen in Fig. 5(b) with

$$E(q) = E_0 + 4\tilde{J}\cos\left(\frac{qb}{2}\right), \tag{2}$$

where $\tilde{J}$ represents the effective interdimer coupling parameter (note that q is parallel to b). This fit is also shown in Fig. 5(b), and we obtained $E_0 = 2.71$ eV and $\tilde{J} = 9$ meV, which gives a total exciton bandwidth of $8\tilde{J} = 72$ meV. We conclude that, in addition to the Coulomb coupling, there

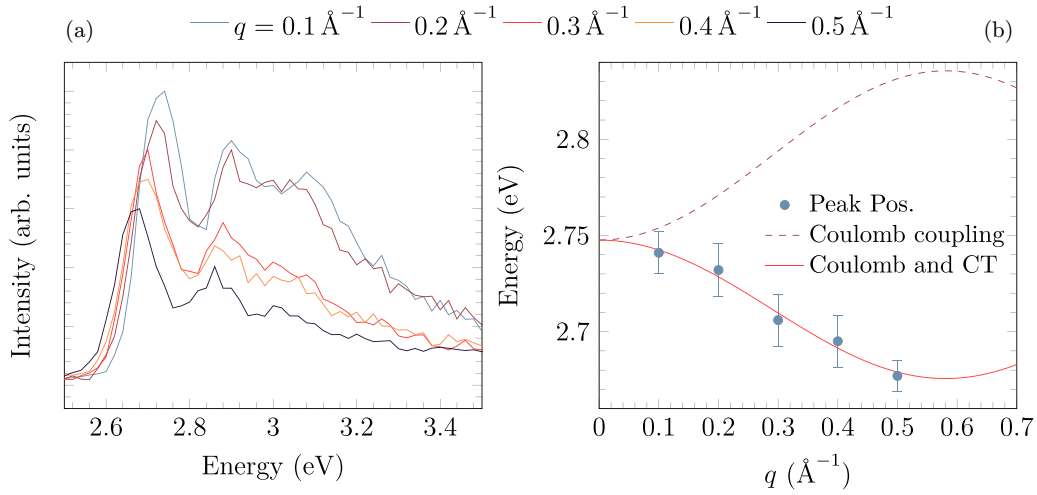

FIG. 5. (a) denotes the exciton dispersion parallel to the crystal b axis as obtained by EELS. A negative dispersion of the first excitation is clearly visible. The energy position of the leading feature in (a) vs the momentum value, as determined by a Gaussian fit (see Supplemental Material [34]) is plotted in (b). The error bars have been taken from the fit results (see Supplemental Material [34]). In addition, we show a fit of the data as outlined in the text (solid line) as well as the expected exciton dispersion based upon Coulomb coupling only (dashed line). We note that the data have been taken in a nonsystematic way in order to avoid an impact of sample damage on the results. Moreover, the data from different samples agree. The cosine fit is outlined in Eqs. (2) and (3) below, and it reflects the interdimer coupling in α-perylene.

must be a second contribution to the interdimer coupling which turns the exciton dispersion for momenta parallel to b negative.

A number of studies of the exciton coupling in various organic materials in recent years indicated that the measured exciton dispersions [35–38] can only be understood when so-called charge-transfer (CT) coupling is considered in addition to the Coulomb term [33,39,40]. Motivated by these results, we introduce an additional interdimer coupling by charge transfer, which in the simplest case would lead to a description of the exciton dispersion by

$$E(q) = E_0 + 4(J_{\text{CT}} - J_C)\cos\left(\frac{qb}{2}\right). \tag{3}$$

Note that J_C is positive. Taking into account the values from above ($J_C = 11$ meV and $\tilde{J} = 9$ meV), this would require a CT coupling J_{CT} of about 20 meV. Following Ref. [6], charge-transfer coupling requires electron and hole exchange (hopping), denoted t_e and t_h, and the charge-transfer coupling in the perturbative regime can be written as

$$J_{\text{CT}} = -2\frac{t_h t_e}{E_{\text{CT}}}, \tag{4}$$

where E_{CT} stands for the energy of the CT state above that of the local exciton. We emphasize that the parameters t_h, t_e, and E_{CT} describe the effective interaction between two dimers. Nevertheless, we can use these in order to analyze whether our simple approach provides a reasonable picture for the exciton behavior in α-perylene.

A band-structure calculation of α-perylene indicates a similar valence and conduction bandwidth W of about 160 meV and an opposite sign of hole and electron transfer [14,41]. Mapping this on the effective hole and electron hopping t_h and t_e would yield ($W = 8t$): $t_e = 20$ meV $= -t_h$. As a consequence, our simple approach would require a charge-transfer energy E_{CT} of 40 meV to reproduce the experimental exciton bandwidth. Our model certainly is too simplistic to arrive at a full quantitative description, but we argue that it nevertheless demonstrates that charge-transfer exciton coupling is present between the dimers of α-perylene, which determines the exciton dispersion as it is the leading contribution as compared to Coulomb coupling. Importantly, it results in a negative exciton dispersion in α-perylene which was unexpected.

Interestingly, it seems unclear to date, how the excitons of the two perylene molecules of the same dimer couple in α-perylene. The picture outlined above predicts strongly Coulomb coupled excitations within the dimer, which was supported by analyses of optical data. However, a recent analysis of the polarization-dependent optical absorption of α-perylene based on many-body perturbation theory within the *GW* approximation and the Bethe-Salpeter equation (BSE) approach came to the conclusion that the lowest, b-polarized exciton in α-perylene is of strong charge-transfer character within a perylene dimer [14], again emphasizing the importance of charge-transfer processes for the exciton physics in molecular crystals in general and in particular in perylene.

V. SUMMARY

Using a space-confined strategy method, 2D single-crystalline α-perylene with a well-controlled thickness has been successfully achieved on a solution surface, which enables a direct transfer to various substrates for further investigations of its structural and electronic properties. Polarization-dependent optical absorption data showed a strong anisotropy in the crystal's ab plane, in good agreement with data from the literature. Electron energy-loss experiments demonstrate that the lowest, optically active exciton is characterized by a negative exciton dispersion along the crystal b axis with an exciton bandwidth of about 72 meV. This exciton dispersion can be rationalized by an effective interdimer coupling with an additional substantial

charge-transfer contribution, which represents the leading term for the exciton delocalization. This emphasizes again the importance of charge-transfer coupling for the photophysical behavior of many organic semiconductors.

ACKNOWLEDGMENTS

We are grateful to M. Naumann, R. Hübel, and F. Thunig for technical assistance. Financial support by the Deutsche Forschungsgemeinschaft within Projects No. KN393/25 and No. KN393/26, the Swedish Research Council (Project Grants No. 2016-05498, No. 2016-05990, No. 2020-04538, and No. 2018-06048), the Swedish Foundation for Strategic Research (ITM17-0432), and the Swedish Government Strategic Research Area in Materials Science on Functional Materials at Linkoping University (Faculty Grant SFO Mat LiU No. 2009 00971) is gratefully acknowledged.

[1] A. Salehi, X. Fu, D.-H. Shin, and F. So, Adv. Funct. Mater. **29**, 1808803 (2019).
[2] H.-W. Chen, J.-H. Lee, B.-Y. Lin, S. Chen, and S.-T. Wu, Light: Sci. Appl. **7**, 17168 (2018).
[3] Z. Hu, J. Wang, X. Ma, J. Gao, C. Xu, K. Yang, Z. Wang, J. Zhang, and F. Zhang, Nano Energy **78**, 105376 (2020).
[4] G. P. Kini, S. J. Jeon, and D. K. Moon, Adv. Funct. Mater. **31**, 2007931 (2021).
[5] M. Riede, D. Spoltore, and K. Leo, Adv. Energy Mater. **11**, 2002653 (2021).
[6] N. J. Hestand and F. C. Spano, Chem. Rev. **118**, 7069 (2018).
[7] N. J. Hestand and F. C. Spano, Acc. Chem. Res. **50**, 341 (2017).
[8] M. Knupfer, T. Pichler, M. S. Golden, J. Fink, M. Murgia, R. H. Michel, R. Zamboni, and C. Taliani, Phys. Rev. Lett. **83**, 1443 (1999).
[9] R. Schuster, J. Trinckauf, C. Habenicht, M. Knupfer, and B. Büchner, Phys. Rev. Lett. **115**, 026404 (2015).
[10] J. van Wezel, R. Schuster, A. König, M. Knupfer, J. van den Brink, H. Berger, and B. Büchner, Phys. Rev. Lett. **107**, 176404 (2011).
[11] A. Camerman and J. Trotter, Proc. R. Soc. London, Ser. A **279**, 129 (1964).
[12] M. Botoshansky, F. H. Herbstein, and M. Kapon, Helv. Chim. Acta **86**, 1113 (2003).
[13] R. M. Hochstrasser, J. Chem. Phys. **40**, 2559 (1964).
[14] T. Rangel, A. Rinn, S. Sharifzadeh, F. H. da Jornada, A. Pick, S. G. Louie, G. Witte, L. Kronik, J. B. Neaton, and S. Chatterjee, Proc. Natl. Acad. Sci. USA **115**, 284 (2018).
[15] J. Tanaka, Bull. Chem. Soc. Jpn. **36**, 1237 (1963).
[16] A. Matsui, K. Mizuno, and M. Iemura, J. Phys. Soc. Jpn. **51**, 1871 (1982).
[17] J. Tanaka, T. Kishi, and M. Tanaka, Bull. Chem. Soc. Jpn. **47**, 2376 (1974).
[18] K. Fuke, K. Kaya, T. Kajiwara, and S. Nagakura, J. Mol. Spectrosc. **63**, 98 (1976).
[19] J. Ferguson, J. Chem. Phys. **44**, 2677 (1966).
[20] A. Witkowski and M. Zgierski, Phys. Status Solidi B **46**, 429 (1971).
[21] Q. Wang, F. Yang, Y. Zhang, M. Chen, X. Zhang, S. Lei, R. Li, and W. Hu, J. Am. Chem. Soc. **140**, 5339 (2018).
[22] L. Zhang, M. M. Hasan, Y. Tang, A. R. Khan, H. Yan, T. Yildirim, X. Sun, J. Zhang, J. Zhu, Y. Zhang *et al.*, Mater. Today **50**, 442 (2021).
[23] F. Yang, S. Cheng, X. Zhang, X. Ren, R. Li, H. Dong, and W. Hu, Adv. Mater. **30**, 1702415 (2018).
[24] X. Huang, D. Ji, H. Fuchs, W. Hu, and T. Li, ChemPhotoChem **4**, 9 (2020).
[25] C. Xu, P. He, J. Liu, A. Cui, H. Dong, Y. Zhen, W. Chen, and W. Hu, Angew. Chem. **128**, 9671 (2016).
[26] A. Virkar, S. Mannsfeld, J. H. Oh, M. F. Toney, Y. H. Tan, G.-y. Liu, J. C. Scott, R. Miller, and Z. Bao, Adv. Funct. Mater. **19**, 1962 (2009).
[27] Q. Liao, H. Zhang, W. Zhu, K. Hu, and H. Fu, J. Mater. Chem. C **2**, 9695 (2014).
[28] H. Jiang, K. K. Zhang, J. Ye, F. Wei, P. Hu, J. Guo, C. Liang, X. Chen, Y. Zhao, L. McNeil *et al.*, Small **9**, 990 (2013).
[29] J. Fink, Adv. Electron. Electron Phys. **75**, 121 (1989).
[30] F. Roth, A. König, J. Fink, B. Büchner, and M. Knupfer, J. Electron Spectrosc. Relat. Phenom. **195**, 85 (2014).
[31] T. J. Kosic, C. L. Schosser, and D. D. Dlott, Chem. Phys. Lett. **96**, 57 (1983).
[32] T. M. Halasinski, J. L. Weisman, R. Ruiterkamp, T. J. Lee, F. Salama, and M. Head-Gordon, J. Phys. Chem. A **107**, 3660 (2003).
[33] N. J. Hestand and F. C. Spano, J. Chem. Phys. **143**, 244707 (2015).
[34] See Supplemental Material at http://link.aps.org/supplemental/10.1103/PhysRevB.107.115201 for the Gaussian fits of the exciton features.
[35] F. Roth, R. Schuster, A. König, M. Knupfer, and H. Berger, J. Chem. Phys. **136**, 204708 (2012).
[36] F. Roth, M. Nohr, S. Hampel, and M. Knupfer, Europhys. Lett. **112**, 37004 (2015).
[37] L. Graf, F. Liu, M. Naumann, F. Roth, B. Debnath, B. Büchner, Y. Krupskaya, A. A. Popov, and M. Knupfer, ACS Omega **7**, 21183 (2022).
[38] L. Graf, Y. Krupskaya, B. Büchner, and M. Knupfer, AIP Adv. **11**, 095313 (2021).
[39] H. Yamagata, J. Norton, E. Hontz, Y. Olivier, D. Beljonne, J.-L. Brédas, R. Silbey, and F. Spano, J. Chem. Phys. **134**, 204703 (2011).
[40] N. Hestand, H. Yamagata, B. Xu, D. Sun, Y. Zhong, A. R. Harutyunyan, G. Chen, H.-L. Dai, Y. Rao, and F. Spano, J. Phys. Chem. C **119**, 22137 (2015).
[41] I. Fedorov, Y. Zhuravlev, and V. Berveno, J. Chem. Phys. **138**, 094509 (2013).